The emergence of social cohesion in a model society of greedy, mobile individuals

Supporting Information

Carlos P. Roca[1] and Dirk Helbing[1,2]

[1] *Chair of Sociology, in particular of Modeling and Simulation,*
ETH Zurich, CH-8092 Zurich, Switzerland,
[2] *Santa Fe Institute, Santa Fe, NM 87501*

1 Introduction

This Supporting Information provides, in the first two sections, further details about the specification and behavior of the model. The last section reports additional simulation results and modifications of the model, carried out in order to verify its robustness.

2 Public Goods Games (PGGs) on networks

Figure SI 1 displays an example of PGGs taking place on a networked population. Individuals correspond to nodes in the network, whereas PGG groups are defined by network neighborhoods. The player in red participates in six PGGs, one centered at herself and five others centered at each of her five neighbors, in blue. The PGG centered at any player comprises the player and all her neighbors. For example, the PGG centered at the red player is held by the six players in color. Typically, players get involved in several PGGs with overlapping but different groups of players.

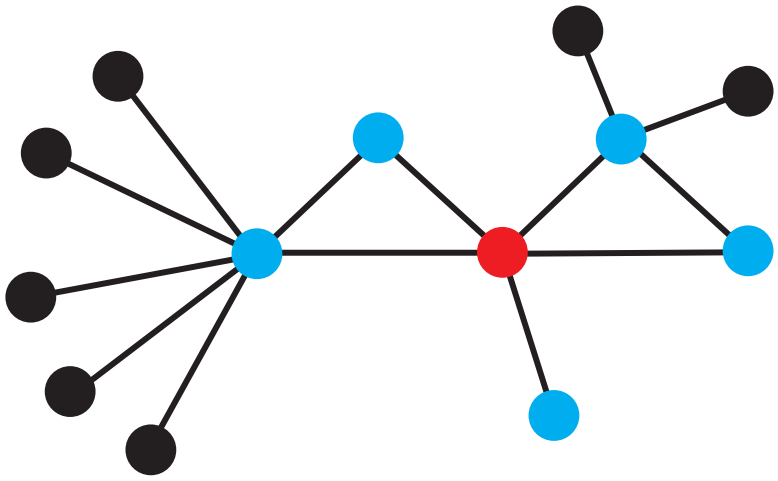

Figure SI 1: Definition of Public Goods Games (PGGs) on networks.

3 Payoff and aspiration evolution

Individuals behave according to a satisficing dynamics, which is defined by means of their satisfaction, by comparing their payoff with their aspiration level (see Eq. [3] of the main text). Aspiration levels, in turn, result from a convex combination of the maximum and minimum perceived payoffs (see Eq. [4]), which feature a habituation effect (see Eqs. [6] and [7]). Figure SI 2 illustrates the evolution of such payoffs and aspiration levels for a typical individual. Notice how the maximum and minimum perceived payoffs (green and blue curves, respectively) follow the evolution of the current payoff (in black). Note also that the payoffs experienced by the individual cover most of the theoretical range between the minimum and maximum attainable payoffs. For a defector this theoretical range corresponds to the interval $[0, rk] = [0, 40]$, whereas for a cooperator it is equal to $[0, (r-1)(k+1)] = [0, 36]$.

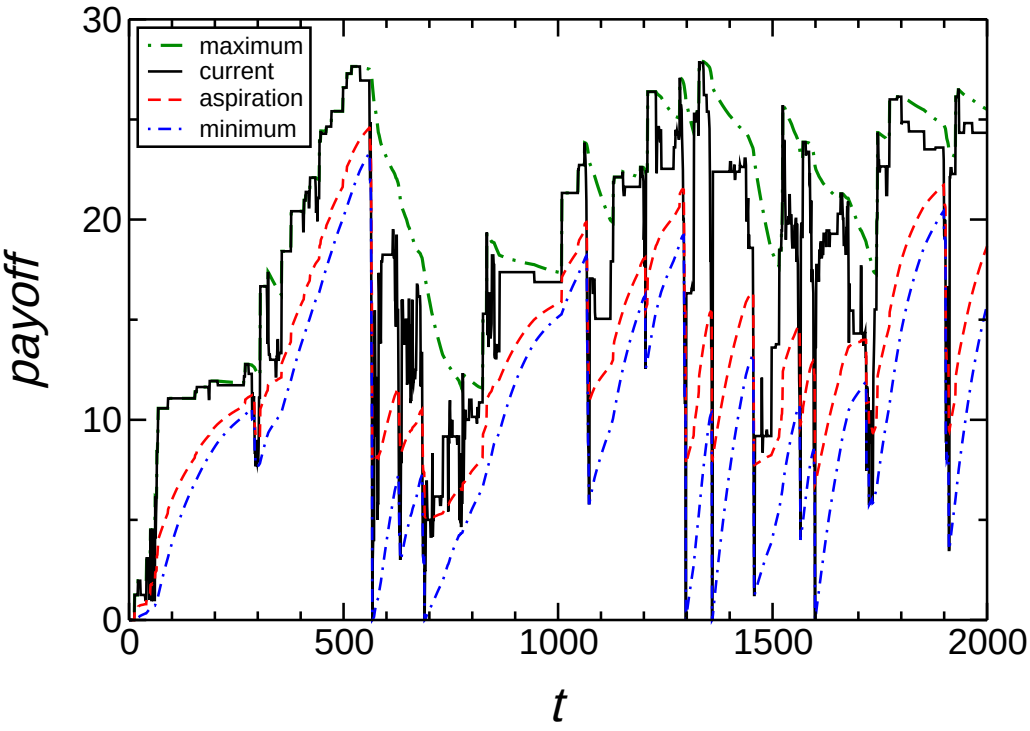

Figure SI 2: Evolution of current, maximum and minimum payoffs, and of the aspiration level for a typical individual (see legend). Model parameters are the same as in Fig. 1 of the main text.

4 Verification of the model robustness

This section presents different modifications of the basic model defined in the main text. Model parameters are the same as in Fig. 1 of the main text, unless stated otherwise. These parameters are repeated in the following for ease of reference.

All subjects are assumed to have the same greediness $\alpha = 0.3$. The synergy factor of the PGGs is $r = 5$, and the underlying network is a half-occupied square lattice of size 10^4, with 8 neighbors (Moore neighborhood). The initial population consists only of defectors, who are randomly distributed over the lattice. The standard deviation of the aspiration noise η is 0.1. The maximum range of migration is $R = 10$. The memory parameter is $\mu = 0.01$. Each cooperator contributes the same quantity 1 to each PGG she participates in.

4.1 System size

Smaller system sizes cause, as expected, larger fluctuations in the time evolution of the population. Figure SI 3 displays several examples. Notice the fluctuations with the smallest size $N = 100$ (black curve). The curves for the largest and second-to-largest sizes, namely $N = 99856$ and $N = 10000$ (red and green curves), virtually overlap.

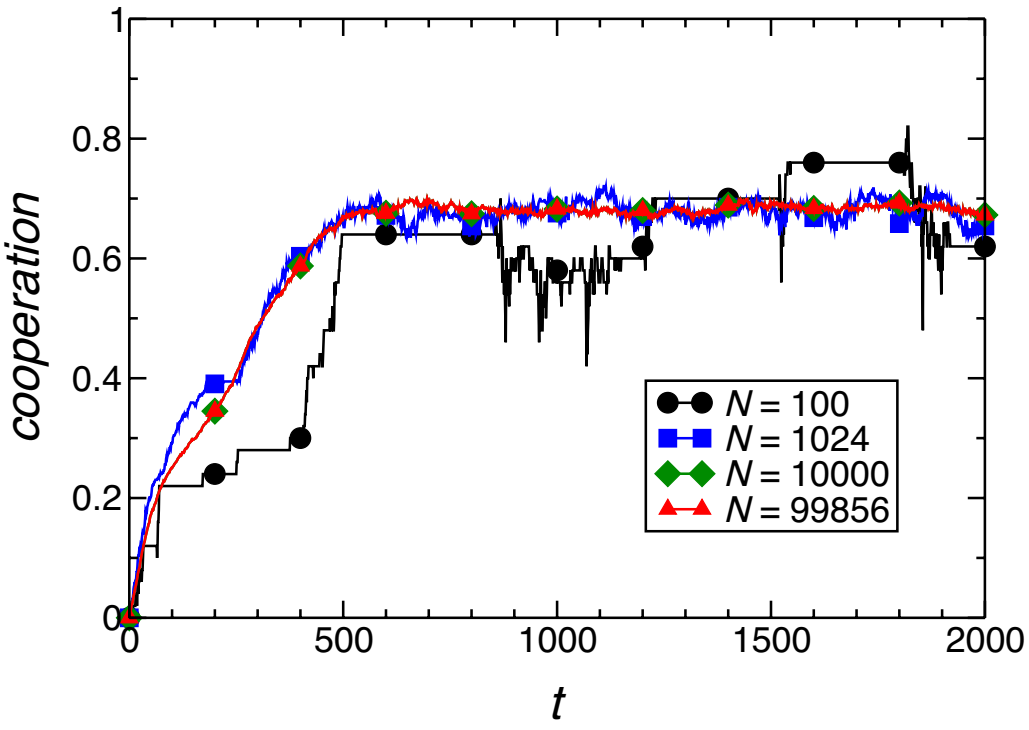

Figure SI 3: Time evolution of the fraction of cooperators in the population, for different sizes of the underlying network N (see legend). Apart from the network size, model parameters are the same as in Fig. 1 of the main text.

4.2 Population density

Figures SI 4 and SI 5 show the stationary state of the model society as a function of the two parameters greediness α and synergy factor r, when the population density is lower or higher than the density considered in the main text, namely 0.25 or 0.75 instead of 0.5. Comparing with Fig. 2 of the main text, it is clear that the main behavior is qualitatively the same. Two differences are, however, worth commenting upon. Cooperation becomes more difficult for higher population densities, as a comparison of panels SI 4B, SI 5B and 2B (main text) reveals. Migration is certainly hindered by higher population densities, so that larger synergy factors r are required to reach a stable and cooperative society. On the other hand, the floor level of aggregation, which corresponds to the random location of individuals, logically depends on the population density, as displayed by panels SI 4C, SI 5C and 2C (main text).

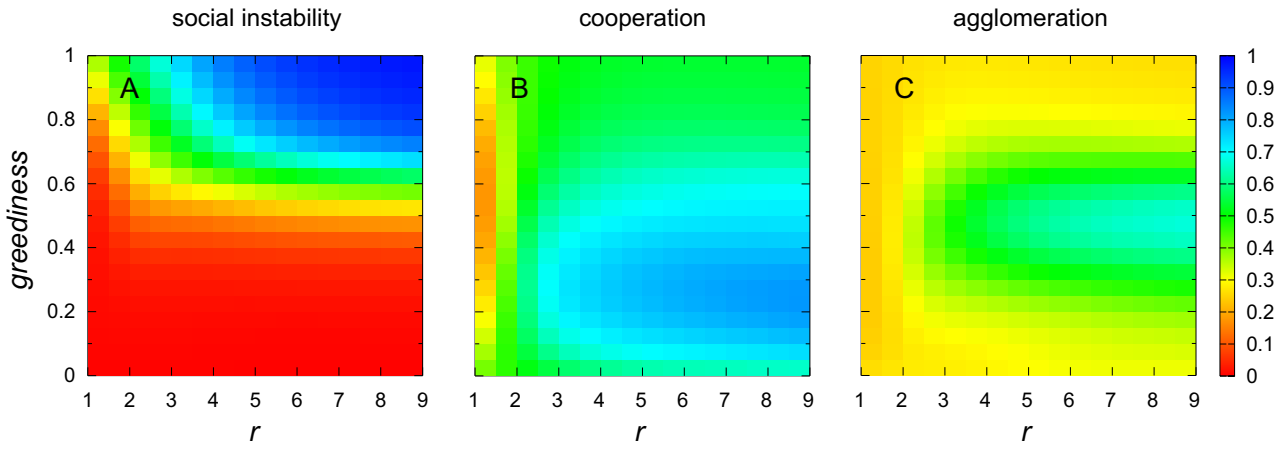

Figure SI 4: Stationary state of the model society, when population density is low (0.25 instead of 0.5). Panels show asymptotic values of the indicated population variables, as a function of the greediness α and the synergy ratio r. The remaining model parameters are the same as in Fig. 2 of the main text.

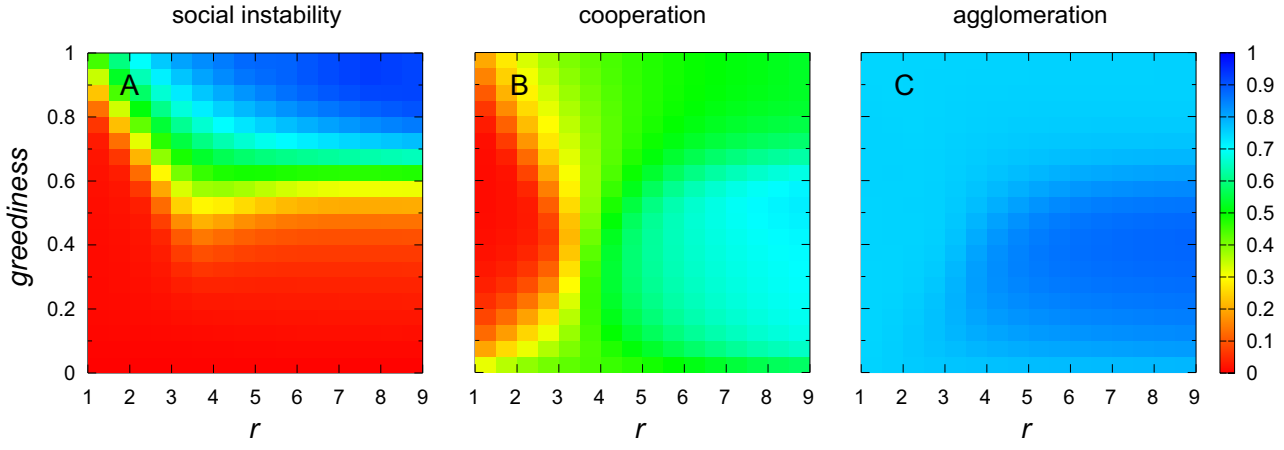

Figure SI 5: Stationary state of the model society, when population density is high (0.75 instead of 0.5). Panels show asymptotic values of the indicated population variables, as a function of the greediness α and the synergy ratio r. The remaining model parameters are the same as in Fig. 2 of the main text.

4.3 Initial fraction of cooperators

The simulations reported in the main text started with an initial population of only defectors. Figure SI 6 shows that the same stationary state is reached regardless of the fraction of cooperators at initial time.

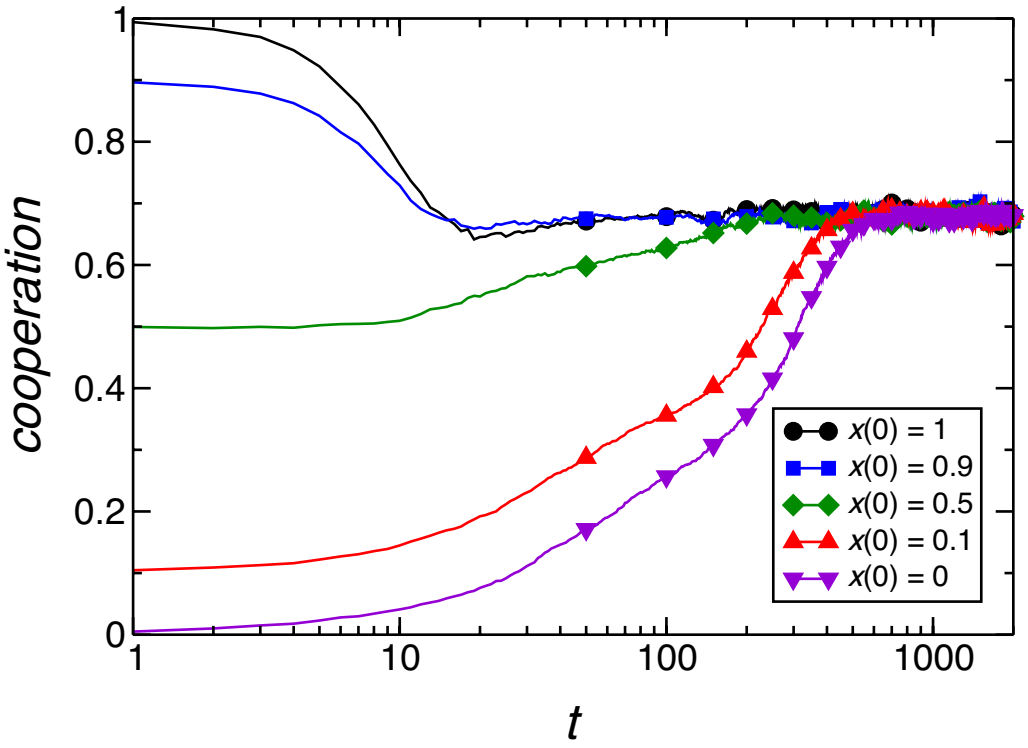

Figure SI 6: Time evolution of cooperation, for different initial fractions of cooperators $x(0)$ (see legend). All other model parameters are the same as in Fig. 1 of the main text.

4.4 Migration range

Figure SI 7 shows that not only the stationary state but also the time evolution is practically independent of the maximum migration range R, provided that this range is large enough. The value of the migration range used for the simulations reported in the main text was $R = 10$.

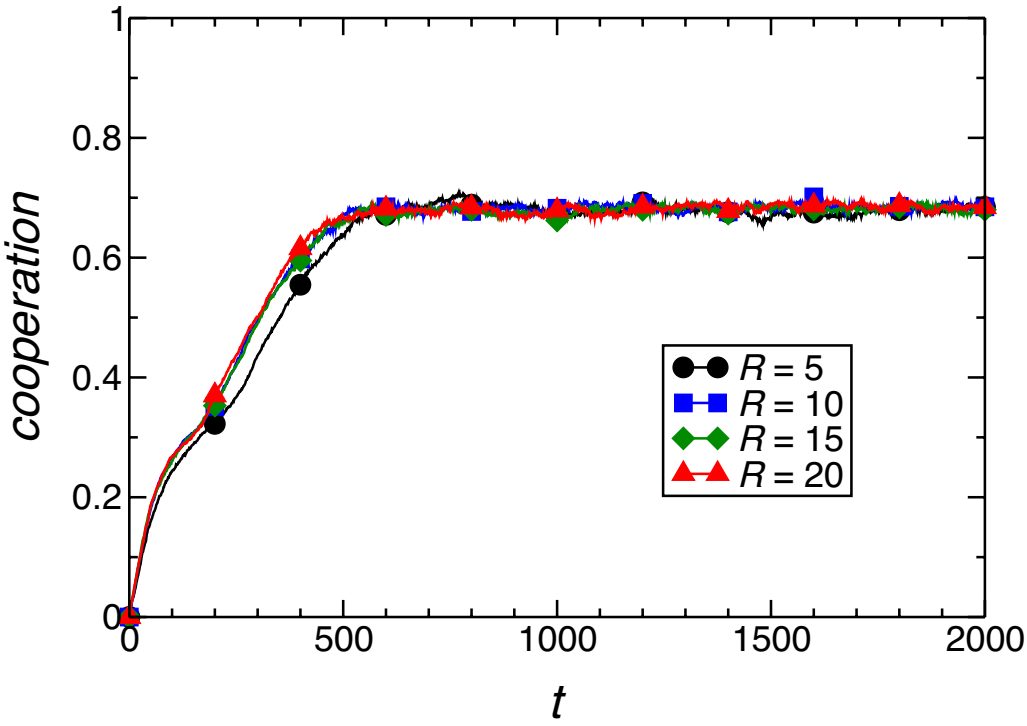

Figure SI 7: Time evolution of cooperation, for different values of the migration range R (see legend). All other model parameters are the same as in Fig. 1 of the main text.

4.5 Network topology

Simulations reported in the main text employed square lattices with 8 neighbors (Moore neighborhood). Figure SI 8 presents results obtained using square lattices with 4 neighbors (von Neumann neighborhood) instead. Compared to Fig. 2 of the main text, the behavior of the model is qualitatively very similar. Notice the different range of the parameter r (synergy ratio of the PGGs), which varies between 1 and $k + 1$.

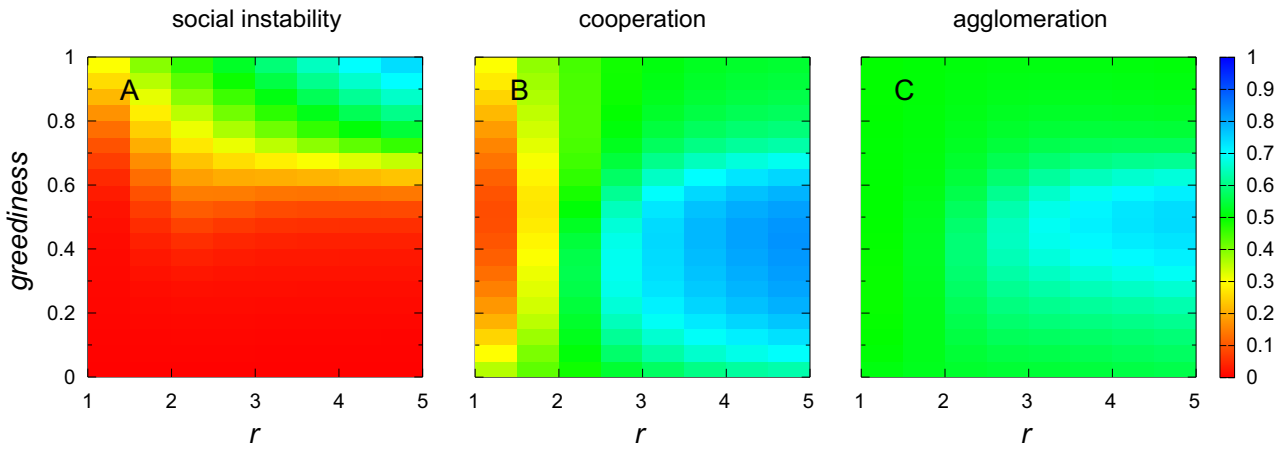

Figure SI 8: Stationary state of the model society, using as underlying network a square lattice with 4 neighbors instead of 8 (von Neumann instead of Moore neighborhood). All other model parameters are the same as in Fig. 2 of the main text.

4.6 Definition of the Public Goods Games

In our definition of PGGs, each cooperator contributes 1 monetary unit to each PGG she participates in. Another option, as explored in [1], is to limit the full amount available for contributions to 1, so that each cooperator gives $1/n$ to each of the n PGGs she is connected to. In contrast to the important differences in results reported in [1], the qualitative outcome of the model is the same in our case, as revealed by the comparison between Fig. SI 9 and Fig. 2 (main text).

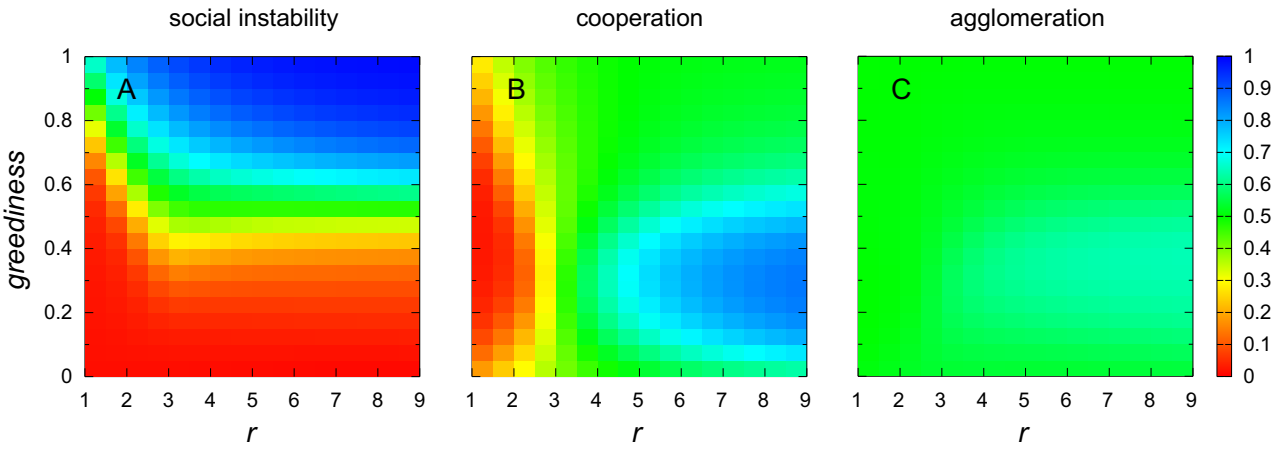

Figure SI 9: Stationary state of the model society, when cooperators contribute $1/n$ (instead of 1) to each of the n PGGs they participate in. Apart from this, all other model features and parameters are the same as in Fig. 2 of the main text.

4.7 Memory length of maximum and minimum payoffs

Individuals in our model society forget the maximum and minimum payoffs they obtain, with a time scale (or memory length) controlled by the parameter μ (see Eqs. [6] and [7] of the main text and Fig. SI 2). The larger the value of μ, the faster they forget (the shortest the memory length). In addition, $\mu = 0$ implies no forgetting (infinite memory length), whereas $\mu = 1$ means instant forgetting (zero memory length).

Figure SI 10 shows that some amount of forgetting (a finite, but larger than zero memory length) is needed for cooperation to emerge. Notice also how the time scale of forgetting has an effect on the convergence to the stationary state. Compare, for example, the cases with $\mu = 0.01$ and $\mu = 0.001$ (green and blue curves).

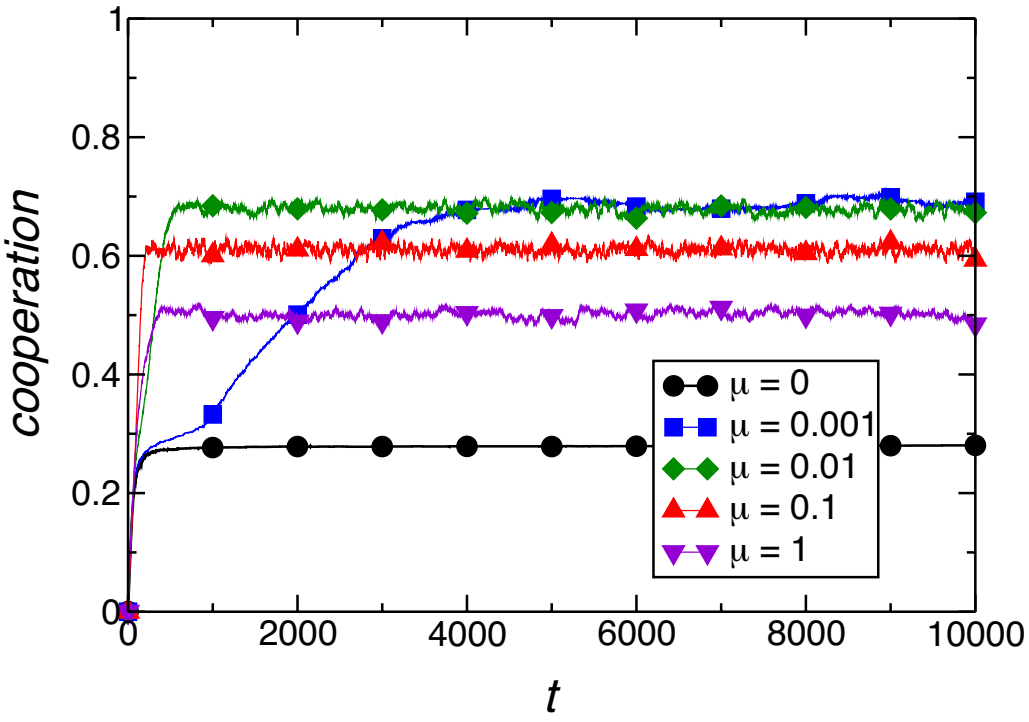

Figure SI 10: Time evolution of cooperation, for different values of the memory parameter μ (see legend). All other model parameters are the same as in Fig. 1 of the main text.

4.8 Aspiration noise

In the simulations reported in the main text, aspiration included a Gaussian noise term with zero mean and standard deviation $\eta = 0.1$ (see Eq. [3] of main text). Logically, some amount of noise is needed for cooperation to emerge in a population comprised only of defectors. Figure SI 11 also shows that larger amounts of noise accelerate the dynamics, but too large noise levels destabilize the model society, making every player behave randomly.

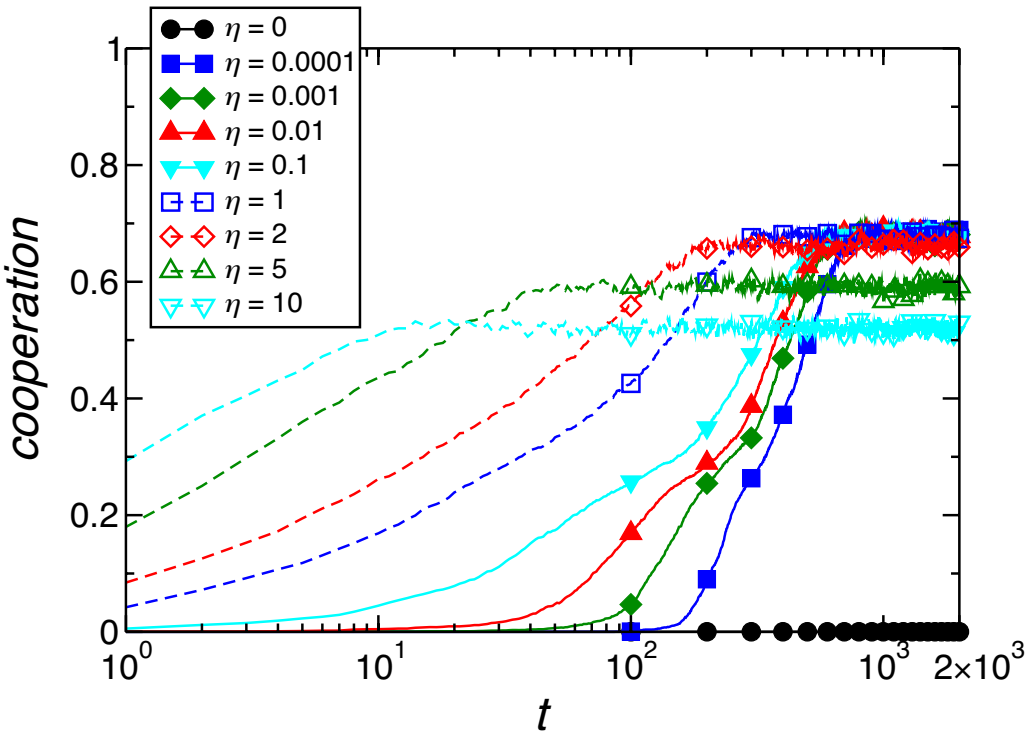

Figure SI 11: Time evolution of cooperation, for different amounts of aspiration noise (see legend, η represents the standard deviation of noise). All other model parameters are the same as in Fig. 1 of the main text.

4.9 Behavioral noise

In order to check the robustness of the decision-making rule followed by individuals, we introduced some behavioral noise in the form of a probability ρ to switch strategy and to migrate to a randomly chosen empty location (with independent random trials), regardless of the individual's satisfaction. The results reported in the main text would correspond to this probability being $\rho = 0$. Figure SI 12 shows that the outcome of the model is robust against this behavioral noise, only displaying a small variation in results as long as the behavioral noise is reasonably low.

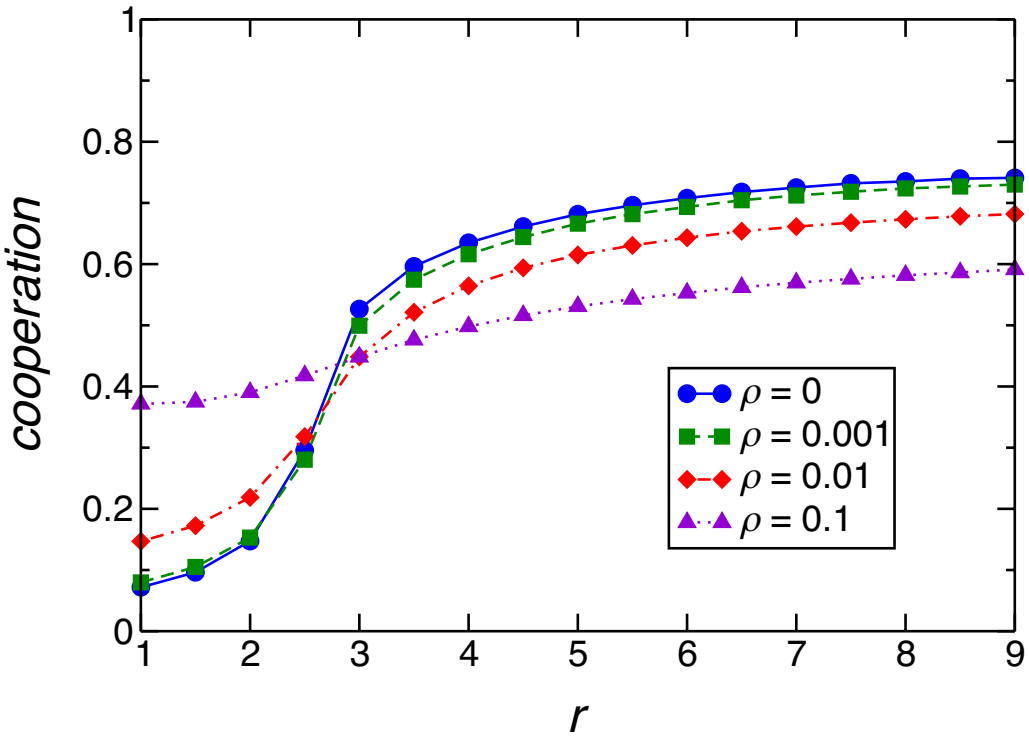

Figure SI 12: Stationary cooperation when individuals switch strategy and/or migrate randomly, regardless of their satisfaction, with probability ρ (see legend). The graph shows the stationary cooperation as a function of the synergy factor r. All other model parameters are the same as in Fig. 2 of the main text, with the exception of greediness, which is set to $\alpha = 0.3$.

4.10 Imitative perturbation of the self-referential learning rule

Another way to check the robustness of the behavioral rule is to introduce a success-biased imitative perturbation, as implemented in [2]. With probability ρ' individuals do not comply with what the learning rule dictates, but they behave following the standard replicator rule, also known as proportional imitation. According to this rule, the individual chooses one of her neighbors at random, compares her payoff with hers and, if the neighbor's payoff is larger, adopts her strategy with a probability proportional to the difference of payoffs (see [2] for full details).

Figure 13 shows that the addition of some amount of imitation to the learning rule only has a minimal effect on the model outcome, provided that the perturbation is small.

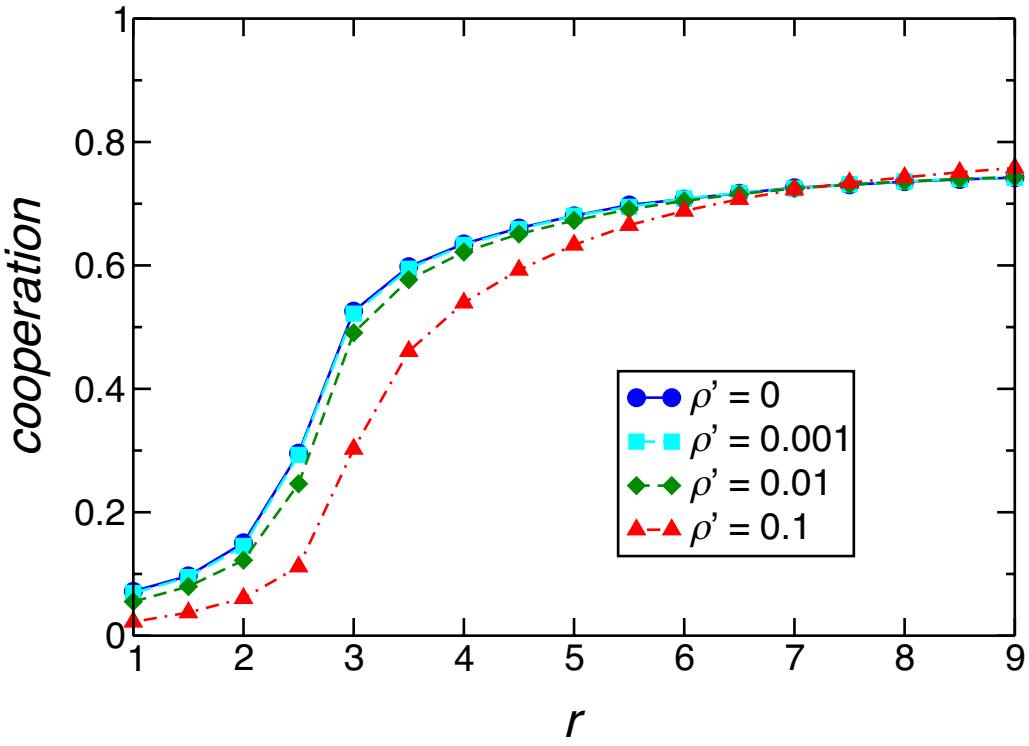

Figure SI 13: Stationary cooperation when individuals imitate more successful neighbors with probability ρ' (see legend). The graph shows the stationary cooperation level as a function of the synergy factor r. All other model parameters are the same as in Fig. 2 of the main text, with the exception of greediness, which is set to $\alpha = 0.3$.

4.11 Ratio between the time scales of migration and strategy change

Individuals in the population update, or decide not to update, both strategy and location after every round of PGGs. This implies that the time scales of location change (migration) and strategy change are the same. It is interesting to study the effect of relaxing this assumption, introducing different probabilities to change location (p_l) and strategy (p_s). The relevant parameter is then the ratio between both probabilities, or its inverse, the ratio between the corresponding time scales, which we define as $\nu = p_l/p_s$. Thus, $\nu = 0$ implies no migration, $\nu = 1$ is the setting of the model in the main text, and $\nu < 1$ ($\nu > 1$) means that migration is slower (faster) than strategy change.

Figure 14 displays simulation results for several time scale ratios. It reveals the crucial impact of migration on the outcome of the model. Compare, for instance, the cases with $\nu \ll 1$ and $\nu = 1$. On the other hand, faster migration improves cooperation for the most demanding PGGs (those with lower r), but in that case it also decreases the stationary cooperation over the full range of r.

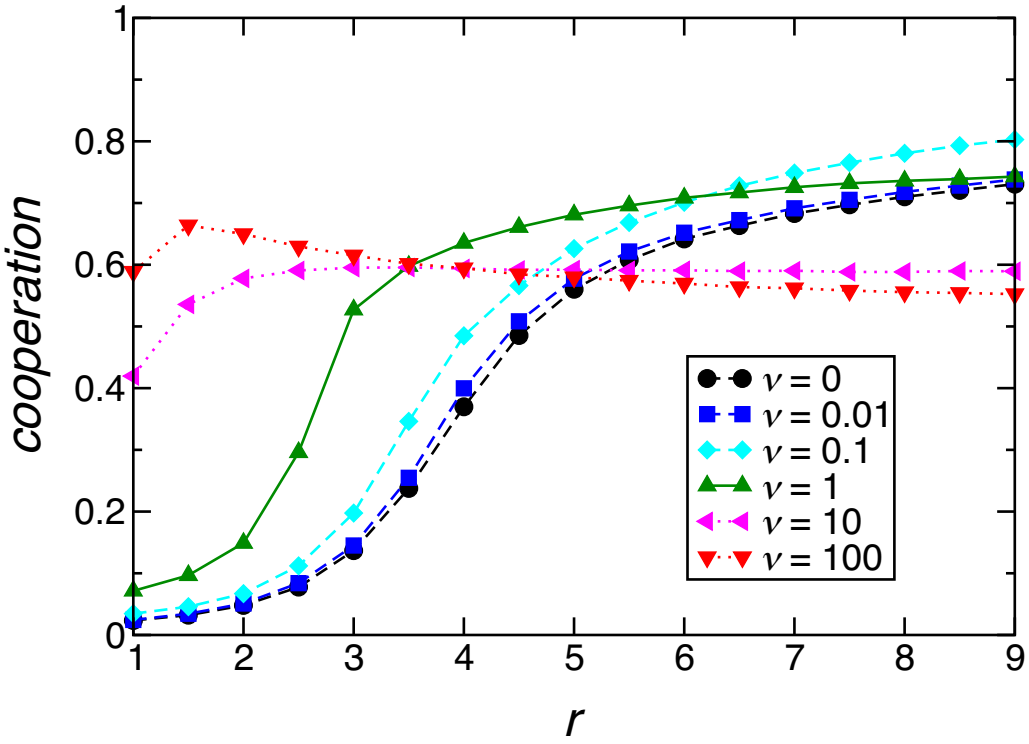

Figure SI 14: Stationary cooperation when individuals migrate with a different time scale than the one with which they update strategy (see legend, ν represents the ratio between both time scales). The graph shows the stationary cooperation level as a function of the synergy factor r. All other model parameters are the same as in Fig. 2 of the main text, with the exception of greediness, which is set to $\alpha = 0.3$.

4.12 Ratio between the time scales of behavioral evolution and greediness evolution

Evolution of greediness was implemented in the main text through a Moran process, with 50 birth-death events between rounds of PGGs and behavioral updates. For a population of 5000 individuals this implies that greediness evolution is $\nu' = 100$ times slower than behavioral evolution. It is always interesting to consider other time scale ratios, which can be easily implemented changing the number of birth-death events between rounds of behavioral updates. For example, 5000 birth-death events make both time scales the same ($\nu' = 1$), whereas 5 birth-death events causes greediness evolution to be $\nu' = 1000$ times slower than behavioral evolution.

Simulation results for different time scale ratios are shown in Fig. 15. On one side, the average greediness converges to similar values, especially when greediness evolution is much slower than behavioral evolution (i.e. for large ν'). On the other hand, faster greediness evolution increases the fluctuations in the evolution of the average greediness. See for example the extreme case with $\nu' = 0.1$, that is, when greediness evolves 10 times faster than behavior.

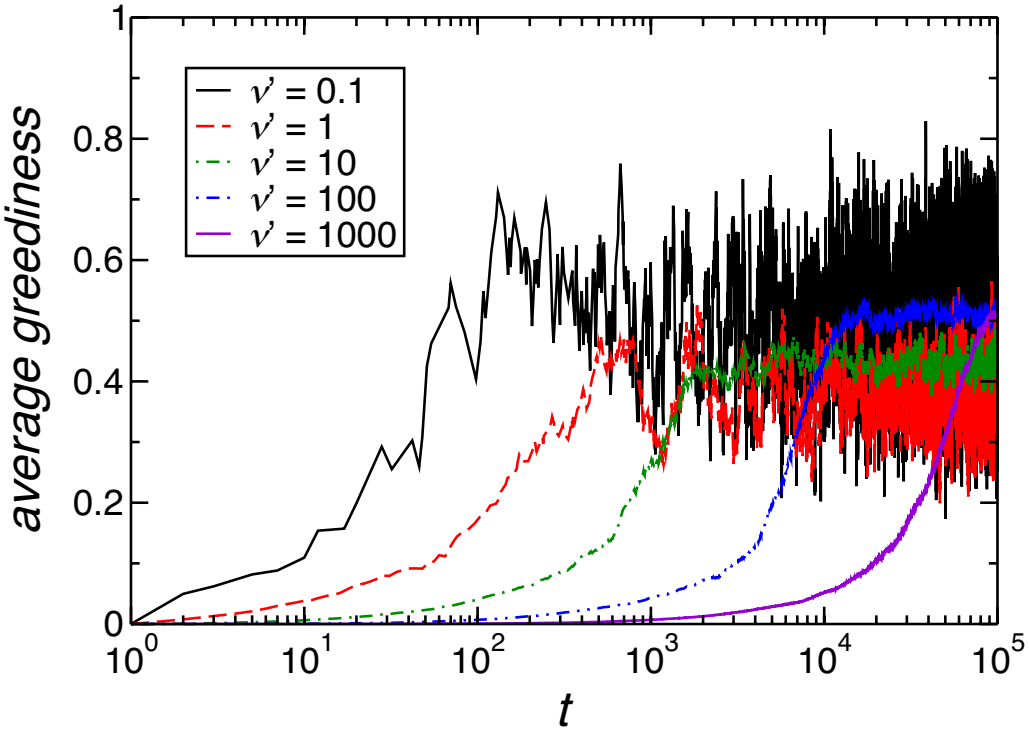

Figure SI 15: Time evolution of the average greediness, when greediness evolves according to a Moran process, for different ratios between the time scales of behavioral evolution and greediness evolution (see legend, ν' represents the ratio between both time scales). Note the logarithmic scale of the abscissa axis (time). All other model parameters are the same as in Fig. 3A of the main text.

References

[1] Santos FC, Santos MD, Pacheco JM (2008) Social diversity promotes the emergence of cooperation in public goods games. *Nature* 454:213–216.

[2] Roca CP, Cuesta JA, Sánchez A (2009) Imperfect imitation can enhance cooperation. *Europhys. Lett.* 87:48005.